Electronic Supporting Information (ESI) for

Multifunctional luminescent magnetic cryocooler in Gd_5Mn_2 pyramid complex

Wei Huang, Shuaidan Huang, Ming Zhang, Yancong Chen, Gui-Lin Zhuang, Yao Li, Ming-Liang Tong,* Juan Yong, Yujie Li and Dayu Wu*

Table of Content

Experimental Sections

Materials and General Procedures. All the reagents employed were commercially available and used without further purification. Methanol and acetonitrile were dried using standard procedures. 1,2-Bis(2-hydroxy-3-methoxybenzylidenne)hydrazine (**H_2L^{OMe}**) was synthesized according to literature method.[1]

Magnetic susceptibility was measured by a Quantum Design MPMS superconducting quantum interference device (SQUID). The derived susceptibilities were corrected for the diamagnetic contribution of the sample, estimated from Pascal's tables.[2] Elemental analyses (C, H, and N) were conducted with a Perkin-Elmer 2400 analyzer. The IR spectra of polycrystalline solids were performed on a Nicolet Magna-IR 750 spectrophotometer in the 4000-400 cm^{-1} region (w, weak; b, broad; m, medium; s, strong) by KBr disc. Solid-state UV-vis spectra were recorded on a SHIMADZU UV-3600 UV−vis−NIR spectrophotometer. Powder X-ray diffraction (PXRD) was recorded on a RINT 2000 vertical goniometer with Cu Kα X-ray source (operated at 40 kV and 100 mA).

Crystal Structure Determination The diffraction intensity data was collected on a Bruker APEX-2 CCD with graphite-monochromated Mo-Kα radiation (λ= 0.71073Å). Data collection, data reduction and cell refinement were performed by using the Bruker Instrument Service v4.2.2 and SAINT V8.34A software.[3,4] Structures were solved by direct methods using the SHELXS program, and refinement was performed using SHELXL based on F^2 through full-matrix least squares routine.[5] Absorption corrections were applied upon using multi-scan program SADABS.[6] Hydrogen atoms of organic ligands were generated geometrically by the riding mode and all the non-hydrogen atoms were refined anisotropically through full-matrix least-squares technique on F^2 with the SHELXTL program package.[7,8] A summary of the crystallographic data and refinement parameters is shown in Table S1.

Fluorescence Measurements The photoluminescence spectra were recorded on an Edinburgh Instruments, Ltd. spectrometer (FS5). All instrument parameters, such as the incident and emergent slit widths (0.2 mm for the incident and emergent slits) and scanning speed (dwell time, 0.5 s; step, 0.5 nm), were fixed for all measurements, and all samples were loaded as soon as possible and sealed in small quartz cells for measurements. The excitation spectra were corrected from 240 to 600 nm for the spectral distribution of the lamp intensity using a photodiode reference detector. Emission and excitation spectra were also corrected for the spectral response of the monochromators and the detector, using typical correction spectra provided by the manufacturer. The measurements at low temperature were performed using a liquid N_2 closed-cycle cryostat. The absolute emission quantum yields were measured at room temperature using a Quantum Yield Measurement System from Edinburgh with a 150 W xenon lamp coupled to a monochromator for wavelength discrimination, an integrating sphere as the sample chamber, and a multichannel analyzer for signal detection. PL decays were recorded using an Edinburgh FLS980 steady state fluorimeter with a time-correlated single-photon counting (TCSPC) spectrometer and a pulsed xenon lamp as the excitation source.

Computational details of Magnetic fitting

Magnetic fitting were conducted by using our home-made programs.[9] In this simulations, we combine the high-performance searching ability of genetic Algorithm with the high-accuracy of Quantum Monte Carlo (QMC).[10] The quantum monte carlo calculation was called by using of the LOOP sub-program of ALPS program.[11] Genetic algorithm details were presented as follows: The whole simulation contains 100 generations. Each population contains 30 chromosomes. The value range of J_1, J_2 and J_3 is set to [-2.0, 2.0] cm^{-1}. In the binary coding process, the accuracy of coupling parameters are set to 1.0×10^{-5}. The genetic operations were performed under the crossover probability (P_c) of 0.80 and mutation probability (P_m) with the value of 0.20. For the QMC computational detail, 2×10^6 Monte Carlo steps (MCS) were used for each site, and the first 10% MCS were discarded for thermalization. All calculations were performed in Guangzhou TianHe-II supercomputer in China.

Essentially, the whole magnetic property of **$\mathbf{Gd_5Mn_2}$** (**1**) was dominated by three type of magnetic exchange: 1) Gd(III)-Gd(III) ions (J_1) doubly bridged by one μ_3-OH and one μ_2-O_{phenolic}, or one μ_3-OH and one N=N bridge; 2) Mn(II)-Gd(III) ions (J_2) by one μ_2-O_{phenolic} and μ_2-$O_{\text{carboxylate}}$; 3) Mn(II)-Gd(III) ions (J_3) by *syn-anti* carboxylate. The Hamilton operator was expressed as following:

$$\begin{aligned} H = -J_1(&S_{Gd1}S_{Gd2}+S_{Gd1}S_{Gd3}+S_{Gd1}S_{Gd4}+S_{Gd1}S_{Gd5}+S_{Gd2}S_{Gd3}+S_{Gd3}S_{Gd4}+S_{Gd4}S_{Gd5} \\ &+S_{Gd5}S_{Gd2}) - J_2(S_{Gd2}S_{\mathrm{Mn1}} + S_{Gd4}S_{\mathrm{Mn2}}) - J_3(S_{Gd1}S_{\mathrm{Mn1}} + S_{Gd1}S_{\mathrm{Mn2}}) \end{aligned} \qquad (1)$$

Negative but small J_1 parameters uncover the anti-ferromagnetic coupling in Gd-Gd, compatible with these observed experimentally and theoretically.[12,13] Also both J_2 and J_3 values exhibit weak anti-ferromagnetic coupling in the propagation of Gd-Mn, consistent with those found in previous GdMn clusters.[14] The weak magnetic exchange lead to the system close to the magnetically isolated one with the large total ground spin for half-filled shell of both Gd^{3+} and Mn^{2+}.

Synthetic procedures

Synthesis of 1,2-Bis(2-hydroxy-3-methoxybenzylidene) hydrazine **(H_2L^{OMe})**

The Schiff base ligand **H_2L^{OMe}** was prepared according to the revised literature method.[1] A mixture solution containing o-vanillin (15.2g,100mmol) and hydrazine hydrate (2.45g, 98%) in 20 mL MeOH was stirred and refluxed for 2h. After cooling to room temperature, the yellow solid was precipitated, filtered and dried in vacuum. Yield: 14.5g (82%). IR (KBr, cm^{-1}): 3438(br), 1629(s), 1469(s), 1255(m), 1080(w), 964(w), 734(s). Elemental analysis (%) calculated for $C_{16}H_{16}N_2O_4$: C, 63.99; H, 5.37; N, 9.33; Found: C, 63.78; H, 5.28; N, 9.31.

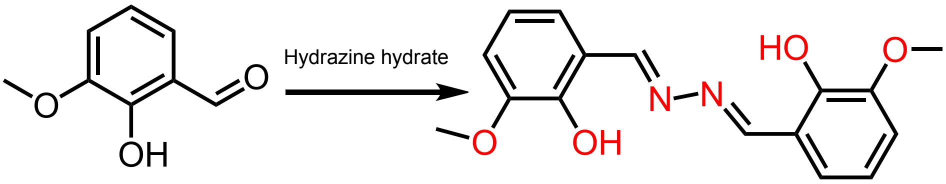

H_2L^{OMe}

Scheme S1. The synthetic route of the target ligand **H_2L^{OMe}.**

Synthesis of complex, **Gd_5Mn_2 (1)**

A mixture of **H_2L^{OMe}** (0.2mmol, 0.06g), $GdCl_3\cdot 6H_2O$ (0.5 mmol, 0.189g) and Et_3N (0.40 mmol, 56μL) in 20 mL of MeOH was stirred for 3 min and $Mn(OAc)_2\cdot 4H_2O$ (0.2 mmol, 0.049g) was then added. The resulting clear yellow solution was stirred briefly and filtered, the yellow block crystals suitable for X-ray diffraction studies were obtained by slow diffusion of ether vapour into the solution after 3 days. Yield: ca. 46%. Elemental analysis (%) calculated for $C_{56}H_{98}Cl_5Gd_5Mn_2N_4O_{36}$: C, 27.16; H, 3.99; N, 2.26; Found: C, 27.56; H, 3.78; N, 2.21; IR (KBr, cm^{-1}) 3403(vs), 2035(m), 1637(s), 1617(s), 1417(m), 1384(m), 1339(m), 1216(w), 1079(w), 981(w), 850(w), 778(m), 617(m).

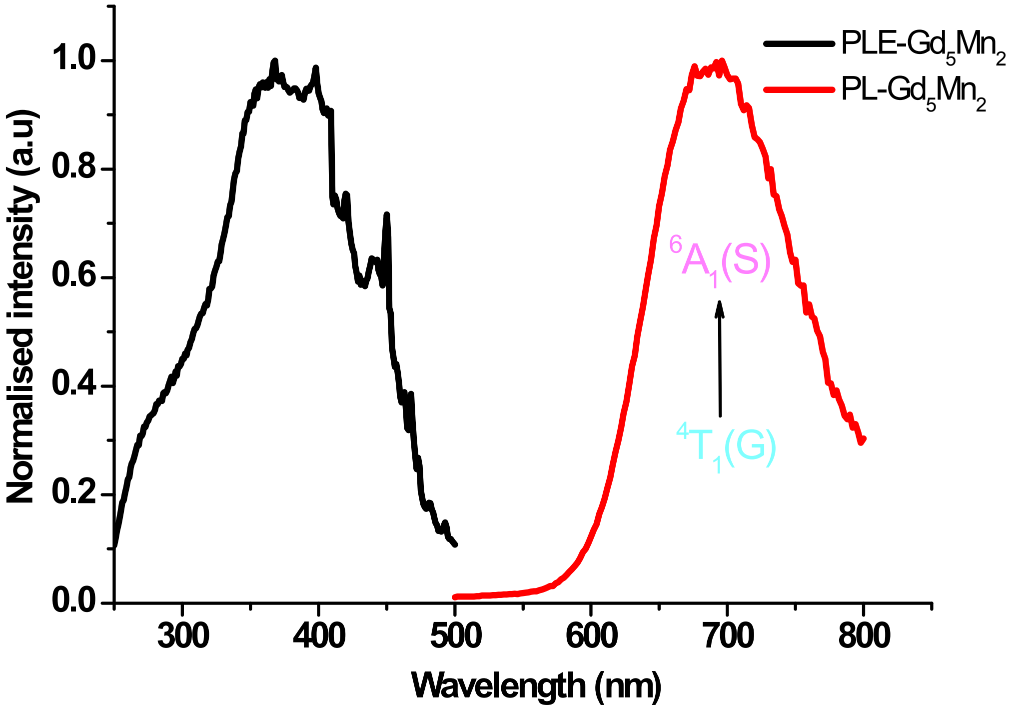

Figure S1. Solid-state emission spectra (red curves) upon photo-excitation at 27400 cm^{-1} (365 nm) and excitation spectra at room temperature (black curves) of **Gd_5Mn_2** (**1**).

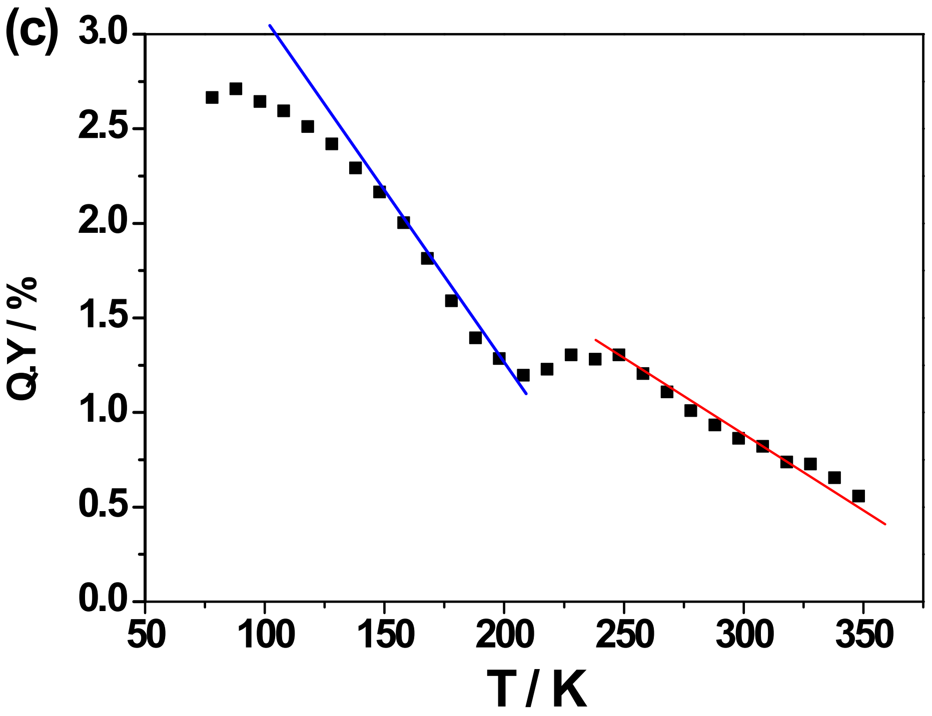

Figure S2. The variation of quantum yield at different temperatures between 77 K an 350 K.

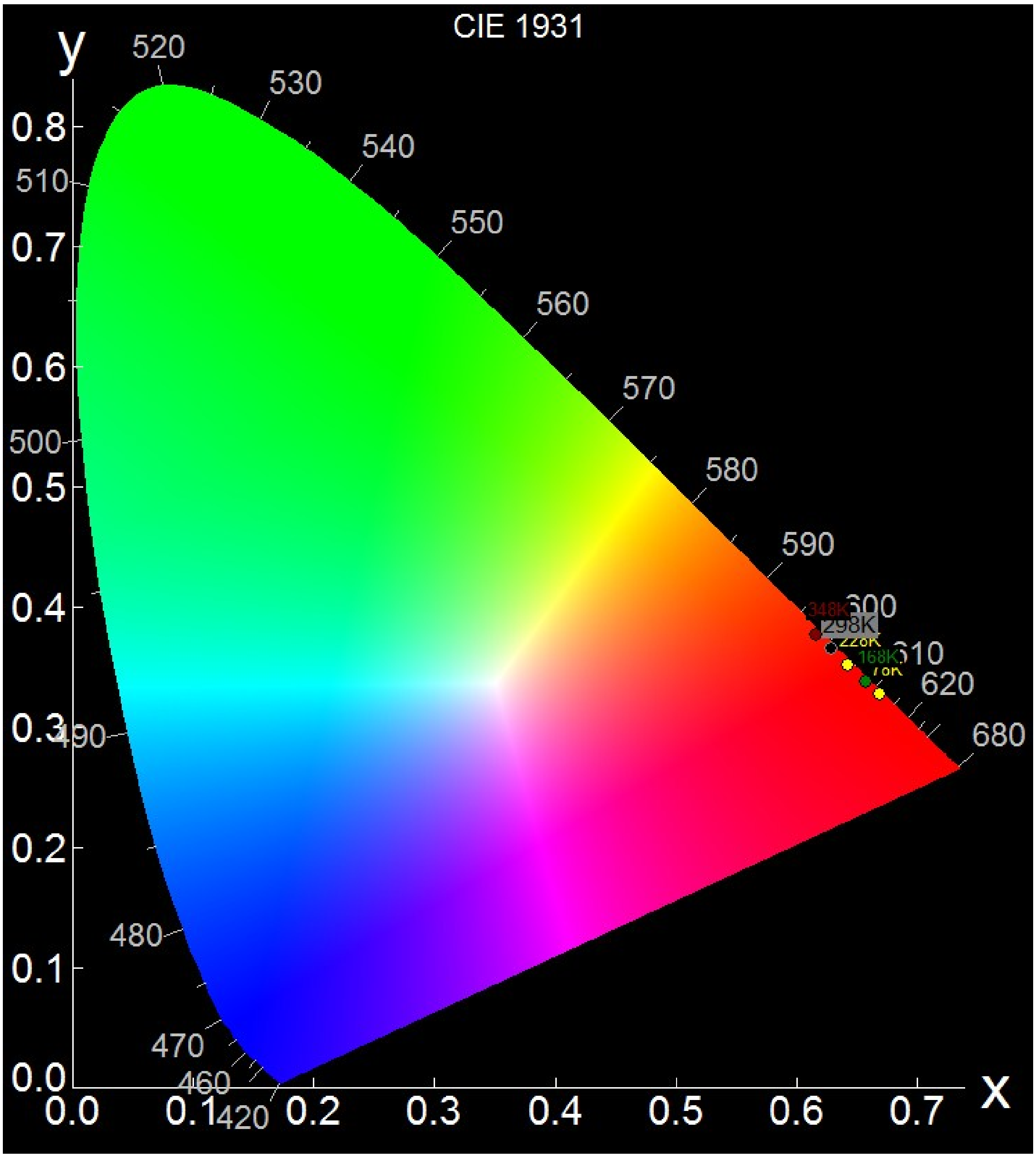

Figure S3. The CIE diagram of compound **Gd_5Mn_2** (**1**) at the selected temperatures between 78 K and 348 K.

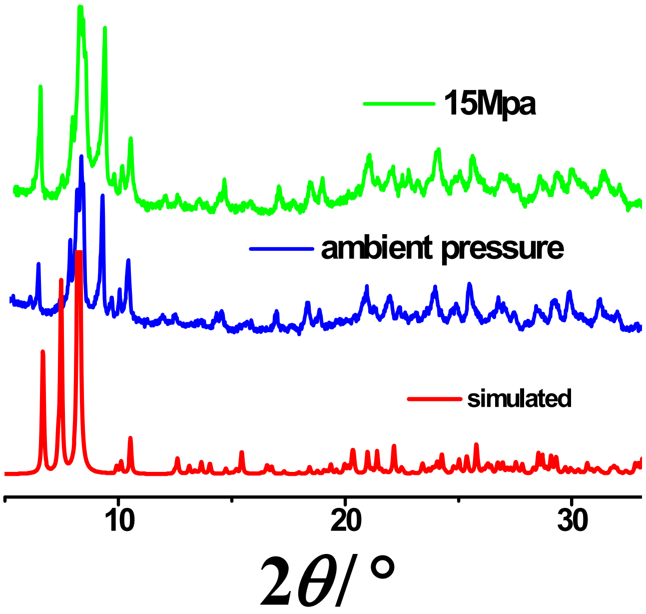

Figure S4. The powder XRD pattern for compound **Gd_5Mn_2** (**1**) before and after pressure.

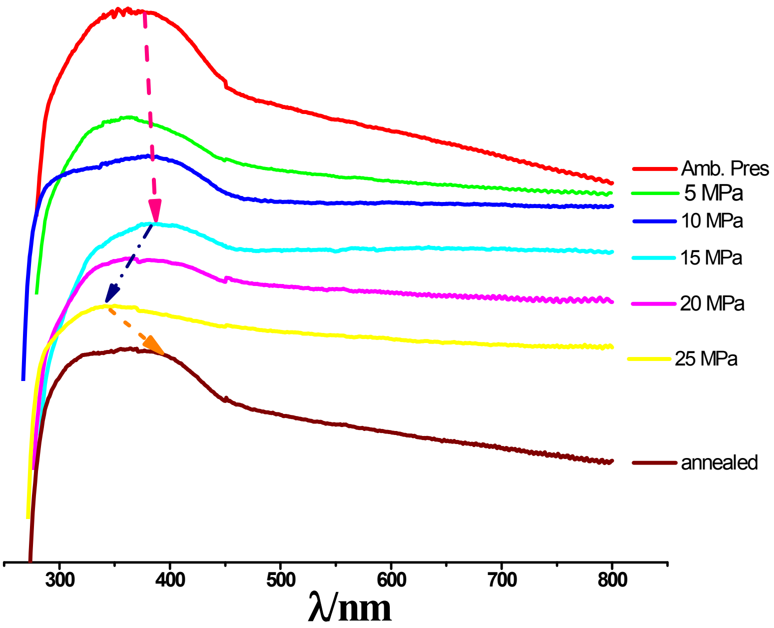

Figure S5. Solid UV-vis spectra of the compound **Gd_5Mn_2** (**1**) that under different pressure.

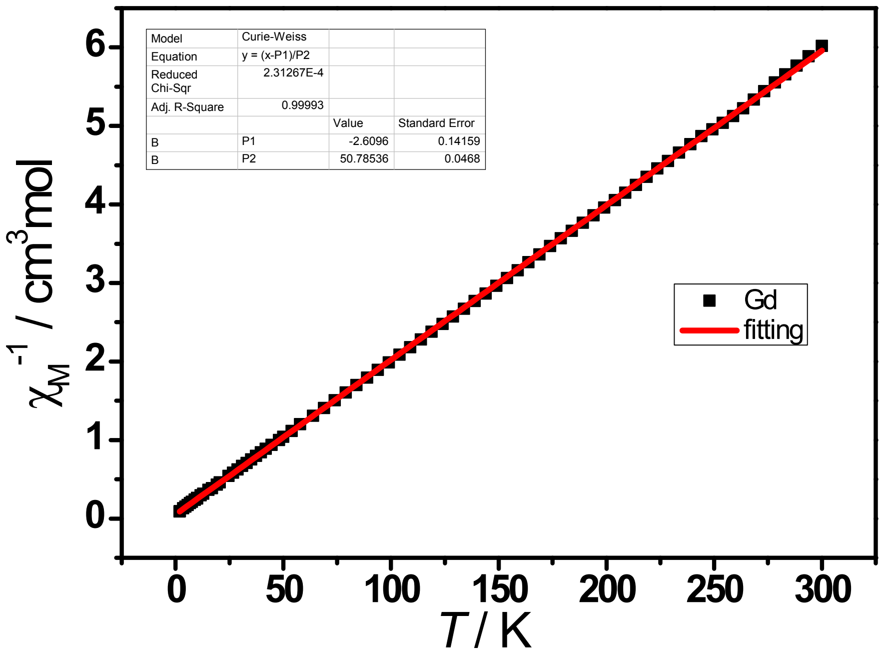

Model	Curie-Weiss		
Equation	y = (x-P1)/P2		
Reduced Chi-Sqr	2.31267E-4		
Adj. R-Square	0.99993		
		Value	Standard Error
B	P1	-2.6096	0.14159
B	P2	50.78536	0.0468

Figure S6. The data of χ_M^{-1} vs T and the fitting of Curie-Weiss laws for compound **Gd_5Mn_2** (**1**).

Table S1. Crystallographic data and structure refinement for **Gd_5Mn_2 (1)**.

Complex	**Gd_5Mn_2(1)**
CCDC No.	1588802
Formula	$C_{56}H_{98}Cl_5Gd_5Mn_2N_4O_{36}$
Mr [g mol^{-1}]	2476.76
Crystal system	Monoclinic
Space group	$C2/c$
Crystal colour	yellow
Crystal description	block
a [Å]	26.495(4)
b [Å]	13.471(2)
c [Å]	23.632(4)
α [º]	90
β [º]	91.092(3)
γ [º]	90
V [Å^3]	8433(2)
Z	4
ρ_{calcd} [g cm^{-3}]	1.951
μ (Mo-K$_\alpha$) [mm^{-1}]	4.405
F (000)	4780
θ range [º]	1.696/24.998
R_1^{a}/wR_2^{b}(I>	0.0550/0.1493
R_1/wR_2(all date)	0.0592/0.1554
GOF^c on F^2	1.080

[a] $R_1 = \sum||F_0| - |F_c||/\sum|F_0|$. [b] $wR_2 = \{\sum[w(F_o^2-F_c^2)^2]/\sum[w(F_0^2)^2]\}^{1/2}$

[c] Goodness-of-fit = $[[w(F_0^2-F_c^2)^2]/(N_{obs}-N_{params})]^{1/2}$, based on the data $I > 2\sigma(I)$.

Table S2. Lifetime τ_1 and τ_2 and the corresponding amplitudes of the components A_1, A_2 of **Gd_5Mn_2 (1)** at 700 nm emissions under interband excitation at 420 nm. Fit parameter deriving from $I(t) = A_1\exp(-t/\tau_1) + A_2\exp(-t/\tau_2)$.

emission	Temp (K)	τ_1 (ns)	B_1 (%)	τ_2 (ns)	B_2 (%)	χ^2
700	300	0.74	4.14	4.38	0.0246	0.88
	200	0.85	3.77	4.60	0.0270	1.20
	100	0.87	3.72	4.47	0.0303	1.13
	77	0.93	3.59	4.47	0.0310	1.42

References:

1 J.-F. Wu, L. Zhao, P. Zhang and J.-K. Tang, Dalton Transactions., 2015. **44**. 11935-11942.

2 O. Kahn, *Molecular Magnetism*; VCH Publishers Inc., 1991.

3 Bruker. SAINT v8.34A. Bruker AXS Inc. 2013 , Madison, Wisconsin, USA.

4 Bruker. APEX2 v2014.5-0. Bruker AXS Inc., 2007 , Madison, Wisconsin, USA.

5 G. M. Sheldrick, Acta Cryst ., 2008 , **64** , 112-122.

6 Bruker SADABS , Bruker AXS Inc. 2014 , Madison, Wisconsin, USA.

7 SHELXTL V5.1, Software Reference Manual; Bruker, AXS, Inc.: Madison, WI,1997 .

8 A. L. J. Spek, Appl. Crystallogr., 2003 , **36** , 7-13.

9 X. Y. Zheng, H. Zhang, Z. X. Wang, P. X. Liu, M. H. Du, Y. Z. Han, R. J. Wei, Z. W. Ouyang, X. J. Kong, G. L. Zhuang, L.S. Long and L. S. Zheng, *Angew. Chem. Int. Ed.*, 2017, 56, 11475-11479.

10 J. H. Holland, Adaptation in natural and artificial system, Ann Arbor, The University of Michigan Press, 1975.

11 A. F. Albuquerque, F. Alet, P. Corboz, P. Dayal, A. Feiguin, S. Fuchs, L. Gamper, E. Gull, S. Gürtler, A. Honecker, R. Igarashi, M. Körner, A. Kozhevnikov, A. Läuchli, S. R. Manmana, M. Matsumoto, I. P. McCulloch, F. Michel, R. M. Noack, G. Pawłowski, L. Pollet, T. Pruschke, U. Schollwöck, S. Todo, S. Trebst, M. Troyer, P. Werner and S. Wessel, *J. Magn. Magn. Mater.* **2007,** *310*, 1187-1193.

12 (a) X. Y. Zheng, Y. H. Jiang, G. L. Zhuang, D. P. Liu, H. P. Liao, X. J. Kong, L. S. Long and L.S. Zheng, *J. Am. Chem. Soc.*, 2017, **139**, 18178–18181;(b) X. Y. Zheng, H. Zhang, Z. X. Wang, P. X. Liu, M. H. Du, Y. Z. Han, R. J. Wei, Z. W. Ouyang, X. J. Kong, G. L. Zhuang, L.S. Long and L. S. Zheng, *Angew. Chem. Int. Ed.*, 2017, **56**, 11475-11479.

13 L. E. Sweet, L. E. Roy, F. Meng and T. Hughbanks, *J. Am. Chem. Soc.* 2006, **128**, 10193-10201.

14 (a) R. Modak, Y. Sikdar, A. Bienko, M. Witwicki, M. Jerzykiewicz and S. Goswami, *Polyhedron*, 2016, **119**, 202-205;(b) Y. F. Bi, X. T. Wang, B. W. Wang, W. Liao, X. Wang, H. Zhang, S. Gao and D. Li, *Dalton Trans.*, 2009, 2250-2254.